# Solvent Effects on the Electronic Spectra: An Extension of the Polarizable Continuum Model to the ZINDO Method

**Marco Caricato***

*Scuola Normale Superiore, Piazza dei Cavalieri 7, 56126 Pisa, Italy*

**Benedetta Mennucci and Jacopo Tomasi**

*Dipartimento di Chimica e Chimica Industriale, Universite di Pisa, via Risorgimento 35, 56126 Pisa, Italy*

*Received: March 12, 2004; In Final Form: April 28, 2004*

We present a method to evaluate absorption energies of a solvated molecule described through a semiempirical wave function. In particular, this paper extends the polarizable continuum model (PCM), in the formulation of the integral equation formalism (IEF), to the ZINDO semiempirical method. The level of theory for the interpretation of the electronic spectra is the Tamm−Dancoff approximation (TDA), using the Hartree−Fock state as reference state. Three different formulas are introduced to calculate the solute−solvent interaction potential. The most relevant formal aspects of the theory are discussed and numerical applications to the study of the transitions from the ground state to the first electronic excited state of some coumarins, of a pyridiniophenoxide betaine molecule, and of the methylene blue dye are presented.

## 1. Introduction

In this paper we present the extension of the solvation model called the polarizable continuum model (PCM)[1,2] to the semiempirical method known as Zerner's intermediate neglect of differential overlap (ZINDO).[3−6] The PCM method was formulated several years ago by Tomasi and co-workers to introduce solvent effects within quantum mechanical (QM) procedures. The PCM method can be easily applied to many levels of QM description and modeled to include various concepts and approaches provided by QM theory.[7] The solute is embedded in a molecular cavity of realistic shape and size inside a continuum dielectric mimicking the solvent, and the corresponding (reaction field) operators are represented through an apparent surface charge (ASC) approach. Many versions of the PCM model have been developed in the past few years; here we shall use the last and most accurate reformulation known as the integral equation formalism (IEF).[8−10] Until now the PCM model has been applied to ab initio methods, and thus its extension to the semiempirical quantum mechanical methods seems to be natural. In fact, at the present time the semiempirical methods are widely used in computational chemistry, in a huge range of applications to phenomena in condensed phase, from the simulation of electronic spectra of solvated systems to the study of reaction mechanisms in biological systems.

Among the semiempirical methods, ZINDO is one of the most popular to perform calculations of electronic excitation energies. It was developed by Zerner, starting from the INDO method, with parameters coming from atomic spectroscopic data, and optimizing the results to reproduce experimental UV spectra. Within the ZINDO scheme, the absorption energies are calculated on the basis of the linear response theory, through the Tamm−Dancoff approximation (TDA), also called the configuration interaction singles (CIS) procedure.

Many attempts have been made to take into account the solvent effects with INDO type methods. The Onsager model,[11] representing the solute−solvent interaction as a dipole−dipole interaction and embedding the solute in a spherical cavity, is often used.[12−14] However, other approaches have been also presented, for which some examples are reported in refs 15−20.

Here we present the first implementation of ZINDO with IEF−PCM. We focus our attention on the electrostatic solute−solvent interaction energy, this being in many cases the most important term. The same approximation was made in all the preceding methods we have quoted.[11−20] The definition of this term depends on the definition of the molecular electrostatic potential (MEP) of the solute. The MEP of a molecule $M$, $V_M(r)$, is the expectation value of a one-electron observable, defined as

$$V_M(r) = \int \Gamma(r')|\, r' - r|^{-1}\, dr' = \sum_{\alpha}^{nuc} Z_\alpha |\, R_\alpha - r|^{-1} - \sum_{\mu\nu} P_{\mu\nu} \langle \mu || r' - r|^{-1} | \nu \rangle \qquad (1)$$

where $\Gamma(r)$ is the solute charge distribution, $Z_\alpha$ is the charge of the nucleus $\alpha$, and we have introduced an expansion of the molecular orbitals on a basis set of atomic orbitals (AO), so that $P_{\mu\nu}$ are the elements of the electronic density matrix on such basis and the terms within brackets are integrals of the $|r' - r|^{-1}$ operator. The analytic expression of $V_M$ given in eq 1 may be replaced by simpler and less costly approximations, especially in connection with semiempirical wave functions. For a comprehensive review we refer to ref 21; here we shall focus on one of the possible strategies, namely that based on the multipole expansion of the MEP.[22,23] This approach introduces approximations because the expansion theorem holds for points $r$ lying outside a sphere containing all the elements of the charge distribution. In molecules, this condition is never exactly satisfied, because the electron charge distribution has an exponential decay. However, the use of multipole expansion

* Corresponding author. E-mail: m.caricato@sns.it.

10.1021/jp048888r CCC: $27.50 
Published on Web 06/17/2004

may reduce the computation time with respect to the MEP analytic expression but still provide a quite accurate description in a large number of cases.

The simplest case of a multipole expansion is given by the expansion limited to the first term, the monopole, represented by proper atomic charges. Many ways can be followed to define atomic charges, among them we quote here the Mulliken population analysis, the so-called potential derived (PD) methods (they start from MEP values, obtained by calculation, and derive atomic charges fitting best the molecular potential),[24] and also experimental methods, introducing "experimental" charges.

In this work, all the approaches just mentioned to compute the MEP (the analytic expression, the multipole expansion, and the atomic charges) will be used in connection with the ZINDO wave function. In this framework, not all the elements of eq 1 must be calculated, because of the zero differential overlap (ZDO) approximation employed in the ZINDO semiempirical method, which reduces further the computational time.

To test our method, a series of calculations on various systems in different solvents are reported. These compounds are: three 7-aminocoumarin dyes, a pyridiniophenoxide betaine and the methylene blue dye. All these molecules are very sensitive to the surrounding medium, and they present a solvatochromic shift in the absorption energies that appreciably depends on the solvent polarity. Many experimental data are present in the literature for these systems. For these reasons they can be taken as valid tests for the reliability of ZINDO/PCM results. Although strong approximations have been introduced in the wave function through a semiempirical method, in the solvent representation through a continuum model, in the MEP calculation, and in the absorption energy evaluation through the TDA procedure, the ZINDO/PCM method is shown to provide results in very good agreement with the experimental data.

This paper is organized as follows. In section 2 the general theory of the ZINDO/PCM method and the implementation details are described. In section 3 we report the numerical applications.

## 2. Theory of ZINDO−PCM

**2.1. IEF−PCM Basic Theory.** In the PCM method[1,2] the solvent S is represented by a homogeneous continuum medium which is polarized by the solute M placed in a cavity built in the bulk of the dielectric. The solute−solvent interactions are described in terms of a solvent reaction potential. This potential, $\hat{V}_{\text{int}}$, is introduced as a perturbation of the Hamiltonian of the isolated molecule, $\hat{H}^0$:

$$\hat{H}_{\text{eff}}\Psi = [\hat{H}^0 + \hat{V}_{\text{int}}]\Psi = E\Psi \tag{2}$$

In eq 2 the Born−Oppenheimer approximation is employed.

In general the solvent-induced term $\hat{V}_{\text{int}}$ is written as a sum of contributions from different physical origins, related to dispersion, repulsion, and electrostatic forces between solute and solvent molecules. In this article we shall focus on the electrostatic part of the interaction only. Within this framework the physics we have to describe is as follows. The solute charge density produces a polarization of the solvent; this polarization is represented by an apparent charge density on the cavity surface which is completely determined by the solute electrostatic potential on the cavity surface, the solvent dielectric constant, and the cavity shape. To simplify the calculation of the solvent apparent charge, the cavity surface is divided into small regions called *tesserae*, with known area. In this way one can approximate the charge density on each tessera as a single-value quantity in order to define the equivalent set of point-like charges. As a consequence the interaction potential can be written in the form

$$\hat{V}_{\text{int}} \rightarrow \sum_{i}^{Nts} q_i \hat{V}_i \tag{3}$$

where $q_i$ and $\hat{V}_i$ are the apparent surface charge and the solute electrostatic potential operator on the tessera $i$, respectively, and the sum runs over the number of tesserae *Nts*. The apparent charges are calculated, using a matrix notation, as[8]

$$\mathbf{q} = \mathbf{QV} \tag{4}$$

where the matrix **Q** depends only on the solvent dielectric constant and on the cavity shape and the vectors **q** and **V** are the vectors of the apparent charges and of the solute potential on the tesserae. Since the solute charge distribution can be divided into nuclear and electronic parts, the same division can be made for the apparent surface charges and for the electrostatic potential, namely

$$q_i = q_i^E + q_i^N \tag{5}$$

$$V_i = V_i^E + V_i^N \tag{6}$$

where the relation between $q^x$ and $V^x$ ($x = E, N$) is given in eq 4.

We shall not go into the details of the computational formulation of the method, for which we refer to refs 8−10, but we focus on the specificities due to the semiempirical description. In the semiempirical framework the differences are in the definition of $\hat{H}^0$, that in our case is the ZINDO Hamiltonian, as implemented in the GAUSSIAN 03 package,[25] and in the definition of the solute electrostatic potential on the cavity surface. The latter definition will be treated in the next section.

**2.2. Interaction Potential.** As shown by eqs. 2−4, in the development of the PCM model in the framework of the ZINDO semiempirical method, the central problem is the calculation of the solute electrostatic potential. The electrostatic potential produced by the solute nuclear charges has a simple form:

$$V_i^N = \sum_{\alpha}^{\text{atoms}} -\frac{Z'_\alpha}{|\mathbf{r}_\alpha - \mathbf{s}_i|} \tag{7}$$

where the nuclear charge $Z_\alpha'$ is reduced for the core electrons and the denominator is the distance modulus between the nucleus $\alpha$ and the center of the tessera $i$.

As shown in eq 1, the electronic potential is represented by a one-electron operator. Because of the ZDO approximation, the one-electron integrals involving two basis functions centered on two different atoms and an operator centered on a third atom are neglected. In the INDO method the one-electron integrals involving two different basis functions centered on the same atom and an operator centered on another atom are also neglected. In the case of PCM the operator $\hat{V}$ is centered on the tesserae, therefore only the one-electron integrals involving the same basis functions centered on the same atom are kept. The following, eqs 8−10 show how the one- and the two-electron

terms of the INDO Fock matrix are modified by the presence of the solvent:

$$F_{\mu\mu}^{AA} = \langle \mu_A | \hat{F} | \mu_A \rangle = h_{\mu\mu}^{AA} + \sum_{i}^{Nts} \langle \mu_A | \hat{V}_i^E | \mu_A \rangle q_i^N + G_{\mu\mu}^{AA}(\mathbf{P}) + \sum_{i}^{Nts} \langle \mu_A | \hat{V}_i^E | \mu_A \rangle q_i^E(\mathbf{P}) \quad (8)$$

$$F_{\mu\nu}^{AA} = \langle \mu_A | \hat{F} | \nu_A \rangle = G_{\mu\nu}^{AA}(\mathbf{P}) \quad (9)$$

$$F_{\mu\nu}^{AB} = \langle \mu_A | \hat{F} | \nu_B \rangle = h_{\mu\nu}^{AB} + G_{\mu\nu}^{AB}(\mathbf{P}) \quad (10)$$

where $\mu_A$ and $\nu_B$ represent two atomic orbitals centered on atoms A and B, and $h$ and $G(\mathbf{P})$ are the one- and two-electron operators of the isolated molecule, respectively (we indicate with the notation ($\mathbf{P}$) the dependence of the two-electron operator $\mathbf{G}$ and of the electronic apparent surface charges $q_i^E$ from the density matrix). We do not show the explicit form of the ZINDO integrals of the isolated molecules and the relative parameterization; the interested reader can find all the details in ref 6. On the contrary, we focus our attention on the PCM integrals: $\hat{V}_i^E$ is the operator of the electrostatic potential induced by the solute electronic charge distribution on the center of the tessera $i$, $q_i^N$ and $q_i^E(\mathbf{P})$ are the apparent surface charges on the same tessera, as defined in eq 5, and the sum runs over the number of tesserae, *Nts*. It is important to stress the difference between $V_i^E$ in eq 6 and $\hat{V}_i^E$ in eq 8: the first one is the expectation value of the electronic potential and it is needed to compute $q_i^E$ according to eq 4; the second one is the corresponding operator. It must be noted that the integrals in eqs 9 and 10 remain unaffected by the introduction of the PCM operators owing to the INDO approximation. In the present paper, three approximated formulas are introduced for the evaluation of the electronic potential and of its corresponding integrals.

*Multip*. The first formula is based on the multipolar expansion of the electrostatic potential integrals $\langle \mu_A | \hat{V}_i^E | \mu_A \rangle$. Within this approach the elementary charge distribution $\mu_A^* \mu_A$ is approximated by a series of point charges: the elements involving two s-type orbitals are represented by a monopole and the elements involving two p-type orbitals are represented by a monopole plus a linear quadrupole:

$$\begin{matrix} ss & r^{-1} \\ p_k p_k & r^{-1} + Q(i)^2 \left( \dfrac{3r_k^2}{r^5} - r^{-3} \right) \end{matrix} \quad (11)$$

where $r$ is the distance between the atom and the center of the tessera and the subscript $k$ represents a Cartesian coordinate. The parameter $Q(i)$ represents the atomic quadrupolar distance for the $i$th element. This kind of approach is used in the NDDO-type methods[26−28] to approximate the electronic charge distribution. For INDO methods, however, the parameters $Q(i)$ have not been calculated; therefore, we have used those obtained for the MNDO method,[29] as implemented in the GAUSSIAN package. This choice is justified by the fact that these parameters will not be very different for ZINDO (as they are not so different between MNDO, AM1,[30] and PM3[31]). As a final comment, we note that the multipole expansion of the potential integrals is exploited also in the calculation of the MEP expectation value $V_i^E$ and in the corresponding apparent charges $q_i^E$.

*Integr*. The second formula explicitly calculates the potential integrals as in the ab initio methods:

$$\langle \mu_A | \hat{V}_i^E | \mu_A \rangle = \left\langle \mu_A \left| \frac{1}{|\mathbf{r} - \mathbf{s}_i|} \right| \mu_A \right\rangle \quad (12)$$

where $|\mathbf{r} - \mathbf{s}_i|$ is the modulus of the distance between the electron and the tessera $i$, and then it excludes the ones that have to be zero for eqs 8−10. Contrary to the previous *Multip* formula, this choice is independent of numerical parameters, but it is computationally more expensive. However, the increment of computational time is not dramatic, therefore we can preserve the advantages of the semiempirical method. As we will show in the application section, the differences of the numerical results between these two options are small and both are close to the experimental ones. Some considerations must be made on the basis set used. Semiempirical methods generally use the minimal basis set, with one s and three p Slater-type orbitals (expanded as STO-6G functions in the GAUSSIAN package). Much attention has been paid to the influence of the basis set in the MEP calculations; the overall conclusion is that the MEP is not heavily affected by the basis set.[21]

*Chg*. Contrary to the previous two formulas, the third one affects only the calculation of the expectation value $V_i^E$ and of the electronic apparent surface charges, $q_i^E$. According to this approach, the electronic charge distribution is described in terms of point charges centered on the nuclei (monopole approximation), and the electrostatic potential acquire a form analogous to the potential produced by the nuclei:

$$V_i^E = \sum_{\alpha}^{atoms} \frac{q_\alpha}{|\mathbf{r}_\alpha - \mathbf{s}_i|} \quad (13)$$

The electronic charge on each nucleus $\alpha$, $q_\alpha$, is calculated as

$$q_\alpha = -e \sum_{\mu \in \alpha} P_{\mu\mu} \quad (14)$$

where $e$ is the electron charge and $P_{\mu\mu}$ are the diagonal elements of the density matrix relative to the atom $\alpha$ in the atomic basis set. This option is often used to compute electrostatic potentials with the INDO method.[18−20] For the calculation of the integrals in eq 8 we use eq 12.

The formulas described in this section are also used in the calculation of the transition energies in the TDA−PCM scheme, treated in the following section.

**2.3. Excitation Energies Calculation.** For the evaluation of the excitation energies we used the Tamm−Dancoff approximation (TDA), also called configuration interaction-singles (CIS).[32,33] This method uses a Hartree−Fock reference state, and it can be seen as a specific case of the more general random phase approximation (RPA). For the development of RPA in the ZINDO framework we refer to refs 14 and 34.

When we are interested in the calculation of excitation energies in condensed phase we need to consider an additional problem not present in isolated systems. The transition to electronically excited states, in fact, involves a dynamical process in which the solvent relaxation time cannot be neglected.[35] One of the most used theories to account for this dynamic effect identifies the solvent response function with a polarization vector depending on time. In most applications, this polarization is divided into two contributions, representing *fast* and *slow* responses. The fast term is associated with the polarization due to the bounded electrons of the solvent molecules, which instantaneously adjust themselves to any

change in the solute charge distribution. The slow term collects many different nuclear and molecular motions in the solvent (vibrational relaxations, rotational and translational diffusion, etc.) related to generally much longer times than those involved both in the change of the solute electronic state and in the solvent electronic polarization. Immediately after a vertical electronic transition, only the fast term will be in equilibrium with the new electronic state. In the PCM scheme this description leads to the definition of two sets of apparent surface charges: the first one (indicated with the subscript f, fast, $\mathbf{q}_f$) depends on the optical dielectric constant of the solvent, $\epsilon_\infty$, and on the charge density of the final solute electronic state, and the second one (indicated with the subscript s, slow, $\mathbf{q}_s$) depends on the static dielectric constant of the solvent, $\epsilon$, and on the charge density of the initial solute electronic state. This delayed solvation is generally known as nonequilibrium solvation.

The nonequilibrium IEF−PCM approach is extensively treated elsewhere;[36−38] here we focus on its formulation within the framework of the TDA−ZINDO scheme.[39] In the TDA scheme, the transition energies are obtained as the solution of an eigenvalue problem of the form[32]

$$\mathbf{M}\mathrm{X}_\mathrm{p} = \omega_\mathrm{p}\mathrm{X}_\mathrm{p} \tag{15}$$

where $\omega_\mathrm{p}$ is the transition energy for the electronic state p and $\mathrm{X}_\mathrm{p}$ is the relative eigenvector.

Including the PCM contribution, the **M** matrix of eq 15 has the form

$$M_{ai,bj} = \delta_{ai,bj}(\epsilon_a - \epsilon_i) + \langle aj||ib\rangle + B_{ai,bj} \tag{16}$$

The spin−orbitals are denoted as follows: *a*, *b* for the virtuals and *i*, *j* for the occupied; $\epsilon$ are the orbital energies (and we have used the Dirac formalism for the antisymmetrized two-electron integrals). As in section 2.2, here we do not show the explicit formulation and parameterization of the ZINDO integrals for the isolated molecule, as reported in detail in refs 6 and 39, but we examine only the PCM terms.

Solvent effects on the excitation energies are present in two ways: implicitly and explicitly. The implicit effect is included in the orbitals and in the orbital energies because of the presence of the PCM operators in the ground-state energy calculation. The explicit effect is represented by the last term on the right-hand side of eq 16; it can be described as the interaction between the solute transition charge density associated with the MO's $|a\rangle$ and $|i\rangle$ and the response of the solvent induced by the parallel transition charge density associated to the MO's $|b\rangle$ and $|j\rangle$. This explicit term can be written in terms of the vector product between the electrostatic potential and the induced apparent fast charges, determined by the corresponding transition density charge, namely:

$$B_{ai,bj} = \mathbf{V}_{ai}\,[\mathbf{q}_f]_{bj} \tag{17}$$

The excitation energy that follows from the solution of the system (15), i.e.,

$$\omega_\mathrm{p} = \sum_{ai}(\epsilon_a - \epsilon_i)X_{ai}{}^2 + \sum_{aibj}[\langle aj||ib\rangle + B_{ai,bj}]X_{ai}X_{bj} \tag{18}$$

includes both solvent effects and it also accounts for the nonequilibrium solvation.

In this paper we do not go into the details of the formal derivation of the TDA procedure within the PCM model, for which we refer to refs 37 and 38, but we stress only the fact that also in this case the PCM fundamental eq 17 depends on the definition of the electrostatic potential. As for the ground-state free energy evaluation, this potential is here calculated following the three approximated formulations described in section 2.2.

Despite the known limits of the TDA approach and the approximation introduced in the interaction potential, ZINDO combined with IEF−PCM offers very good results for the transition energies, as shown in the next section. Sometimes they are better than those obtained with ab initio methods, in addition to being much less time demanding.

These three options, as implemented in a local version of the GAUSSIAN 03 development code, were tested on a series of compounds for which experimental data are available. The results are reported in the numerical section.

## 3. Numerical Applications

In this section we present some applications of the ZINDO/PCM approach to a series of compounds for the calculation of transition energies from the ground state to the first singlet excited state. The aim is to compare the semiempirical results with the experimental data and with ab initio results. Moreover, a comparison of the timings between the gas phase and the solution calculations and between the three options for the potential evaluation are reported in section 3.1.

In section 3.2 three different coumarin dyes are studied into two solvents, the first one apolar (cyclohexane) and the second one polar and aprotic (acetonitrile); in section 3.3 the system studied is a betaine in a series of solvents with increasing polarity; in section 3.4 calculations performed with different methods on the methylene blue dye in water solvent are compared.

The cavity is built as usual, through interlocking spheres centered on atoms; the hydrogen atoms bonded to carbon atoms are included in the spheres of the carbons. The radii of the spheres are $R_\mathrm{F} = 1.67$ Å for fluorine atoms, $R_\mathrm{O} = 1.82$ Å for oxygen atoms, $R_\mathrm{N} = 1.86$ Å for nitrogen atoms, $R_\mathrm{C} = 2.04$ Å for carbons without bonded hydrogen, $R_{\mathrm{C1}} = 2.28$ Å for carbons with one bonded hydrogen, $R_{\mathrm{C2}} = 2.40$ Å for carbons with two or three bonded hydrogens, and $R_\mathrm{H} = 1.44$ Å for hydrogens not bonded to a carbon.

The geometries of all the compounds were obtained with the AM1/PCM optimization method that we have recently implemented in the same local version of GAUSSIAN 03 code. In AM1/PCM the definition of the potential integrals is obtained in terms of a multipolar expansion, as in the option *Multip*, using the correct parameters for the AM1 method.[30]

**3.1. Timing.** Before going into the details of the numerical applications, some consideration about the timing of the calculations should be taken. The inclusion of the solvent effect in the calculation obviously leads to an increase of the computational effort. In the case of PCM this increment principally depends on the evaluation of the electrostatic potential, eq 6, and on the solution of the system in eq 4 for the evaluation of the apparent surface charges. This system is usually solved through the technique of the matrix inversion, which scales as the square of the number of the tesserae.

In ab initio calculations, the increment due to the PCM is of the same order of magnitude needed for the evaluations of the integrals of the gas-phase Hamiltonian. This condition is no longer true in the semiempirical framework. In fact, although the interaction potential evaluation is simplified through the approximations introduced in section 2.2, the solution of the system (eq 4) still depends on the square number of the tesserae, through the inversion of the matrix **Q**. Thus the relative increase of the computational time passing from gas phase to solution

calculations is much more evident in the semiempirical framework than in the ab initio one.

Here we do not report the timing for all the compounds, but we report just some comments. The calculations were carried out with a Pentium IV 2.0 GHz machine. For the betaine molecule, which is the smallest system, the order of magnitude of timing passes from 10 s in the gas phase to 10−20 min in different solvents (with the option *Multip*, which is the fastest one). In this case the number of tesserae is of the order of 1450 (the number of tesserae varies with the shape of the cavity, which depends on the equilibrium geometry of the solute in the various solvents). In the case of the coumarin 153, which is the largest system, the timing passes from 30 s in the gas phase to 130 min in solution (still with the option *Multip*), with the number of tesserae ∼1800. However, we note that other factors can influence the speed of a calculation, such as the convergence of the SCF or the evaluation of the transition energies, which can be different in the various solvents, thus the values reported are only indicative.

Despite that the relative increase of the timings for the calculations in solution is relevant, it is important to stress that ab initio calculations in solution still remain much more expensive (and, as we shall show below, not necessarily closer to the experimental data). For example, in the calculation of coumarin 153 at the level B3LYP/6-311+G(d), the timing is of the order of 5600 min, and thus ZINDO/PCM calculations are ∼45 times faster.

Moreover, we recall that another method has been recently developed for the calculation of the apparent surface charges,[40] based on the fast multipole method (FMM). This method iteratively solves the system in eq 4 and linearly scales with the number of the tesserae. Although we did not use this method in the present work (the compounds studied here are in fact relatively small), it can be used with ZINDO/PCM and it surely represents the most efficient approach for larger molecules. All these considerations should be sufficient to state that, by using PCM with the semiempirical methods, one does not lose the advantages of the velocity of these methods.

Another important consideration can be made about the relative timing between the three approximations introduced in section 2.2 for the calculation of the electrostatic potential. We found that the *Multip* option is the fastest one, followed by the *Chg* option (from ∼10% to ∼30% slower than the *Multip*), and finally by the *Integer* option (from ∼20% to ∼55% slower than the *Multip*). We note that these differences also depend on the number of the tesserae: the difference decreases with increasing the number of the tesserae. The reason is that by increasing the surface of the cavity (and the number of tesserae), the effort of solving eq 4 becomes more important than the evaluation of the potential, and this fact leads to a leveling of the performances of the three options.

For this paper we chose systems small enough to be treated at an ab initio level, and this fact allowed us to compare different levels of QM theory. Comparing the different options used for the evaluation of the potential, we can see that, considering the computational time, the best one is the *Multip* option, which also provides, in the large number of systems, the values of transition energies closest to the experimental data, as it will be shown in the next sections.

**3.2. Coumarins.** The 7-aminocoumarins[41−44] are an important class of laser dyes for the blue-green region because of their strong absorption cross sections and large radiative yields. The energy of the lowest singlet excited state relative to the ground state is quite sensitive to the substituents on the amine function and also to the polarity of the environment (due to the dipole moment change between the ground and the excited state). There is a large interest in the absorption and emission spectra of this class of molecules, therefore, many data, measured and calculated, are available for systems with different substituents and in various solvents.

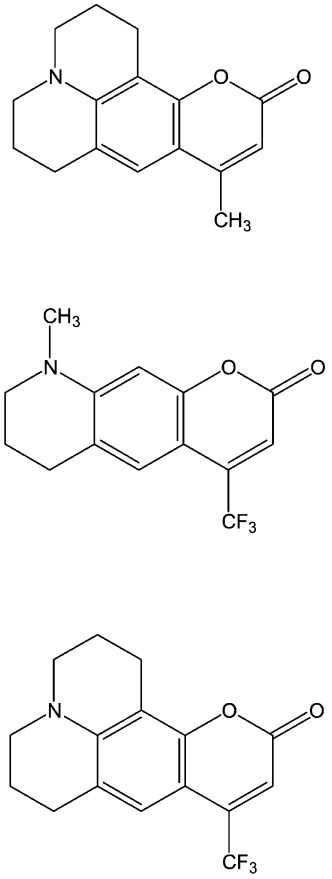


**Figure 1.** Molecular structures of the three coumarins. Top: coumarin 102; center: coumarin 522; bottom: coumarin 153.

Here we present the calculations on three different coumarins (see Figure 1). The absorption energies and their dependence on the solvent polarity are studied and comparisons with experimental data and with the TD-DFT/PCM calculations are presented.

For coumarins 102 and 522, the calculations were performed in cyclohexane (dielectric constant $\epsilon = 2.02$) and in acetonitrile ($\epsilon = 36.64$); for coumarin 153, only in acetonitrile. The experimental[42] and the ZINDO/PCM results are reported in Tables 1−3. For the ZINDO/PCM, three sets of data are reported, corresponding to the three different options we have implemented; the notation is the same as defined in section 2.2. For coumarin 153, the TD-DFT/PCM results (using the B3LYP functional, a 6-311G(d) basis set for the geometry optimization, and a 6-311+G(d) basis set for the transition energy evaluation) are also reported.

The experimental data show a red shift of absorption wavelength with increasing solvent polarity; all three ZINDO/PCM options reproduce correctly this trend. Tables 1−3 also show that the difference among the three alternative ZINDO/PCM options is at most 0.08 eV, with the results obtained with the *Integr* and *Chg* options being very close to each other. With respect to the experimental data, the option *Multip* in general gives the best results, very close to the experimental results for the more polar solvent (acetonitrile). For the apolar solvent the results are worse, probably because the approximation to

**TABLE 1: Absorption Energies (eV) for Coumarin 102 in Two Different Solvents[a]**

| 102 | acetonitrile | cyclohexane |
|---|---|---|
| exp. | 3.26 | 3.43 |
| Multip | 3.21 | 3.34 |
| Integr | 3.21 | 3.26 |
| Chg | 3.20 | 3.26 |

[a] Calculations performed with the three options of the ZINDO/PCM method.

**TABLE 2: Absorption Energies (eV) for Coumarin 522 in Two Different Solvents[a]**

| 522 | acetonitrile | cyclohexane |
|---|---|---|
| exp. | 3.06 | 3.25 |
| Multip | 3.04 | 3.15 |
| Integr | 2.98 | 3.07 |
| Chg | 2.98 | 3.08 |

[a] Calculations performed with the three options of the ZINDO/PCM method.

**TABLE 3: Absorption Energies (eV) for the Coumarin 153 in Acetonitrile[a]**

| 153 | absorption energy |
|---|---|
| exp. | 2.97 |
| TD−DFT | 2.95 |
| Multip | 3.00 |
| Integr | 2.95 |
| Chg | 2.94 |

[a] Calculations performed with the three options of the ZINDO/PCM method and with the TD−DFT/PCM method (B3LYP, 6-311+G(d) basis set).

**TABLE 4: Absorption Energies (eV) for the Coumarins Reported in Figure 1 in Vacuo and in Acetonitrile (option *Multip*)[a]**

| | vacuum | PCM | exp. |
|---|---|---|---|
| 102 | 3.48 | 3.21 | 3.26 |
| 522 | 3.34 | 3.04 | 3.06 |
| 153 | 3.31 | 3.00 | 2.97 |

[a] In all cases the geometries are those optimized with the AM1/PCM in acetonitrile.

consider only electrostatic solute−solvent interaction is too strong in this case. However, the experimental trend of the transition energies, passing from the polar solvent to the apolar one, is well reproduced.

As far as coumarin 153 is concerned, the TD-DFT/PCM and the ZINDO/ PCM results are similar and they both well agree with the experimental data.

To achieve a more detailed analysis of the PCM effect on the spectra, in Table 4 we report the ZINDO results obtained for the three coumarins in vacuo and with PCM (acetonitrile, option *Multip*), at the geometries optimized in acetonitrile with the AM1/PCM method. In this way we have separated the solvent effect on the geometries from that on the absorption energies. As shown in the table, the results in vacuo are systematically too large with respect to the experimental data. In contrast, the use of PCM provides energy values in very good agreement with the experimental values, correctly reproducing the stabilization effect of the solvent on the solute electronic excited state.

**3.3. Betaine.** Also the family of pyridiniophenoxide betaines is the subject of considerable interest because of their solvatochromic properties.[45−49] In fact, the most famous member of this class, the betaine 30, was used for the definition of a polarity scale (called the $E_T(30)$ scale) of wide application.[50] The solvent sensibility of the absorption spectra is due to the fact that the excited state involves a charge transfer (CT) from the phenoxide donor ring to the pyridinium acceptor ring. The stabilization of this CT state with respect to the ground state and the position of the band in the spectrum are largely affected by the solvents as well as the nature of the substituents on the rings. In this article we focus our attention on the unsubstituted molecule, see Figure 2, so to avoid the effect of substituents and leave only that of the solvent.

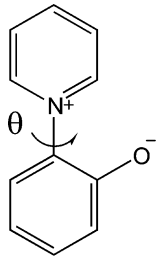


**Figure 2.** Molecular structure of the betaine molecule. Torsional angle $\theta$ between the two rings.

**TABLE 5: Dielectric Constants ($\epsilon$) and Dihedral Angle $\theta$ (degrees) for the Betaine Molecule in Vacuo and in Solvent of Increasing Polarity, Obtained by Geometry Optimizations with AM1 and B3LYP/6-311G(d) Methods and PCM**

| | $\epsilon$ | AM1 | DFT |
|---|---|---|---|
| vacuum | 1 | 30.8 | 31.5 |
| benzene | 2.25 | 34.0 | 35.8 |
| $CHCl_3$ | 4.90 | 36.2 | 38.8 |
| $CH_2Cl_2$ | 8.39 | 37.3 | 40.3 |
| acetone | 20.7 | 38.1 | 42.2 |
| acetonitrile | 36.64 | 38.3 | 42.7 |
| $CH_3OH$ | 32.6 | 38.3 | 41.8 |
| water | 78.39 | 38.7 | 42.7 |

We performed calculations in a series of solvents with increasing polarity. Contrary to the previous collection of systems, presenting a quite rigid geometrical structure, in this system one immediately recognizes a critical geometrical parameter, namely the dihedral angle $\theta$ between the rings (see Figure 2). To have a better analysis of the importance of this parameter and of its changes according to the solvent, in Table 5 we report the values of $\theta$, obtained by geometry optimizations performed with the AM1 and B3LYP (6-311G(d) basis set) methods in vacuo and in different solvents. Table 5 also reports the dielectric constants $\epsilon$ of the solvents.

From the analysis of the results reported in Table 5 it comes out that $\theta$ increases with the solvent polarity to a saturation value for the most polar solvents. It can be noted that the semiempirical method provides values of $\theta$ quite close to those obtained with the DFT method; this fact makes us confident of the accuracy of the AM1 geometries. This confidence is also confirmed by other studies on similar compounds, performed with different computational methods and solvation models, in which a similar gas-to-solvent change of the dihedral angle is found.[49]

The values of $\theta$ have been then used to compute absorption energies in the different environments. Table 6 shows the results for the absorption energies in vacuo and in solvents with the three ZINDO/PCM options, the experimental data,[47] and the calculations performed with TD-DFT/PCM (B3LYP/6-311+G-(d)). Each system has been studied at the geometry optimized in the corresponding phase.

It can be noted that the ZINDO result in vacuo is quite far from the experimental data in the solvents, so the use of PCM becomes necessary to correctly reproduce the measured absorption energies.

Except for the less polar solvent (benzene) and for the protic solvents (methanol and water), which we will examine more

**TABLE 6: Absorption Energy (eV) in Vacuo and in Various Solvents for the Betaine Molecule[a]**

| | exp. | Multip | Integr | Chg | TD−DFT |
|---|---|---|---|---|---|
| vacuum | | | 1.83[b] | | 2.08 |
| benzene | 2.35 | 2.03 | 1.98 | 1.98 | 2.06 |
| $CHCl_3$ | 2.40 | 2.33 | 2.31 | 2.30 | 2.14 |
| $CH_2Cl_2$ | 2.49 | 2.48 | 2.46 | 2.46 | 2.19 |
| acetone | 2.55 | 2.60 | 2.57 | 2.57 | 2.22 |
| acetonitrile | 2.60 | 2.65 | 2.63 | 2.63 | 2.24 |
| $CH_3OH$ | 3.03 | 2.64 | 2.63 | 2.63 | 2.24 |
| water | 3.28 | 2.69 | 2.67 | 2.66 | 2.25 |

[a] Calculations performed in vacuo with ZINDO and TD-DFT (B3LYP/6-311+G(d)) methods and in solvent with the three options of the ZINDO/PCM and with the TD-DFT/PCM (B3LYP/ 6-311G(d)) methods. [b] Calculation in vacuo provides only a single value.

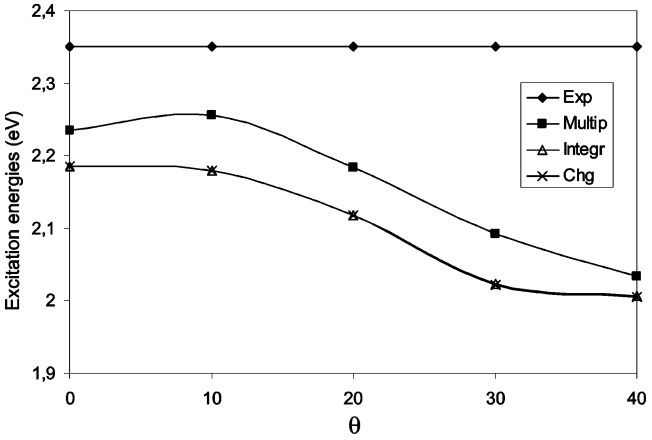


**Figure 3.** Absorption energies (eV) diagrammed as a function of the dihedral angle $\theta$ (degree) for the betaine molecule in benzene, evaluated with the three options of the ZINDO/PCM method. The experimental energy value is plotted as reference.

accurately following this section, for all aprotic solvents the differences between ZINDO/PCM results and experimental data are smaller than 0.1 eV. The *Integr* and *Chg* options still give results very close to each other and numerically smaller than the *Multip* option, which still gives the best results.

The comparison of ZINDO and TD-DFT calculations is also of interest. In fact, for the latter method the results are worse than for the former. This example clearly testifies to the validity of the ZINDO/PCM method, which, despite the approximations it introduces in the QM description, can give results more in agreement with the experimental data than the ab initio one.

The ZINDO/PCM result becomes worse in benzene, but the result is not improved by increasing the level of the calculation and passing to the TD-DFT/PCM method. As for the coumarins, also in this case an electrostatic-only description of the solute−solvent interaction seems to be a too strong approximation. This fact can also be reflected in the geometry, and, for example, the value of $\theta$ obtained with the algorithm accounting only for the electrostatic term could be not correct. To check this issue we performed a series of calculations of absorption energies at different dihedral angles, starting from the geometry optimized in benzene with the AM1 method, keeping the other internal coordinates fixed. The results are reported in the diagram of Figure 3.

As shown in the diagram, probably the value of $\theta$ obtained in the geometry optimization (34°) is too large but, even varying this parameter, the calculated absorption energy remains still quite far from the experimental value. This fact seems to show that nonelectrostatic effects should be explicitly introduced in the calculation of the excitation energies as well as accounted for in the determination of the geometry. We also note that the

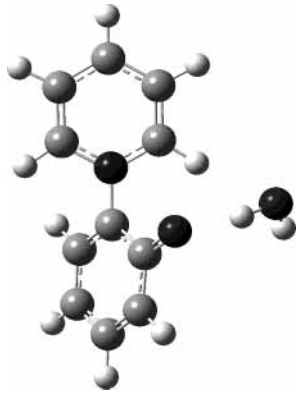

**Figure 4.** Structure of the betaine + *explicit* water molecule system. The water molecule is H-bonded to the oxygen atom of the betaine.

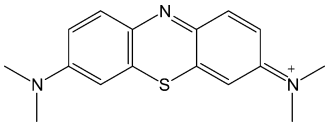


**Figure 5.** Molecular structure of the methylene blue cation.

**TABLE 7: Betaine + One *Explicit* Water Molecule, Absorption Energy (eV) Calculated in Vacuo and in Water[a]**

| | absorption energy |
|---|---|
| exp. | 3.28 |
| vacuum | 1.83 |
| Multip | 2.89 |
| Integr | 2.89 |
| Chg | 2.88 |

[a] Geometry optimized in water with B3LYP/PCM (6-311G(d) basis set).

diagram again reveals that the *Integr* and *Chg* results are very close to each other, but that the *Multip* option provides the best performance.

Examining the results for the protic solvents, we can guess that the hydrogen bond has an important role for this system (that presents intramolecular charge separation), but this contribution cannot be well described with a continuum-only model. This deficiency can be reduced by inserting one or more *explicit* solvent molecules H-bonded to the oxygen atom. Choosing water as the test case (for methanol the results should be analogous), we performed the absorption energy calculations in water, adding one explicit water molecule, see Figure 4.

The geometry of the H-bonded 1-water betaine system was optimized using the B3LYP/ PCM (6-311G(d) basis set), because it is known that the AM1 does not give reliable hydrogen bonding distances. In Table 7 we report the absorption energies calculated in vacuo and in water (with the three options) at the same geometry ($\theta = 48.3°$).

From this table one can see that the presence of the explicit water molecule improves the performance of ZINDO/PCM. In contrast, for the calculation in vacuo the absorption energy value is not influenced at all. This strange behavior is due to two opposite effects: the increase of torsional angle $\theta$, due to the presence of the water molecule, tends to decrease the value of the transition energy with respect to the isolated molecule and, on the other hand, the polarization effect of the same water molecule tends to increase this value. In the calculation in vacuo, these two effects cancel each other and we obtain the same result as obtained for the isolated molecule (see Table 6). In the PCM calculation, the polarization effect due to the explicit water molecule is stronger, providing a significant net increase of the absorption energy with respect to the value reported in Table

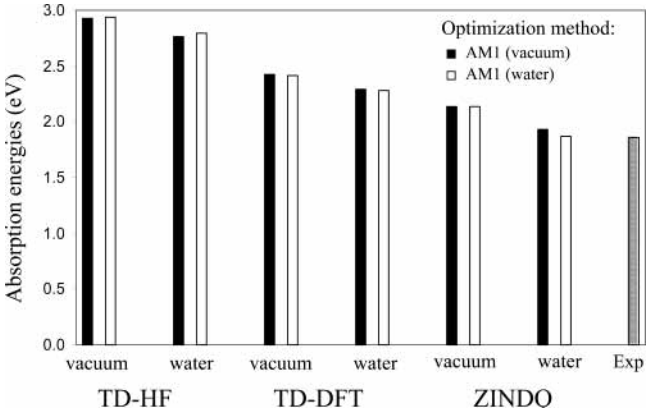


**Figure 6.** Absorption energies (eV) for the methylene blue dye. The geometry was optimized in vacuo and in water with the AM1 method. The absorption energies were evaluated in vacuo and in water with the ZINDO, TD−HF (6-31+G(d) basis set), and TD−DFT (B3LYP, 6-31+G(d) basis set) methods. For ZINDO/PCM, the *Multip* option was used.

6. To verify that in water the geometrical effect does not strongly influence the values of the transition energies, we performed calculations with PCM and in the presence of the explicit water molecule changing the angle $\theta$ (and keeping fixed the other internal coordinates). From these calculations we found that the transition energies do not vary significantly with respect to the values reported in Table 7.

From the comparison of the PCM results of Tables 6 and 7, we can see that the discrepancy found in water with respect to experiments is significantly reduced, however, it remains larger than in aprotic solvents. The addition of a second H-bonded water molecule does not change the description, and thus we are led to think that this remaining discrepancy is due to an intrinsic limit of the ZINDO method to correctly describe the effect of H-bonds.

To summarize the results of this section, we can see that, when the most important part of the solute−solvent interaction is electrostatic, the semiempirical PCM approach to the absorption energy evaluation is very good, providing results very close to the experimental results, even better than those obtained with ab initio methods.

**3.4. Methylene Blue.** Methylene blue is a cationic dye (see Figure 5) largely used in different fields. We quote here its use in the treatment of various diseases, as a dye in surgical and medical marking, and as an indicator dye.[51] In the latter case its interactions with clay minerals are widely examined;[52−55] in these studies visible spectra of dye−clay suspensions in water are reported, as are the spectra of dilute solutions.[55] In this paper we analyze the absorption spectra of the methylene blue, comparing different methods, ab initio and semiempirical, with respect to each other and the experimental data.[53]

In Figure 6 we report a diagram showing the experimental absorption energy compared with those obtained with TD-HF, TD-DFT, and ZINDO methods, in vacuo and in water. The geometries optimized in vacuo and in solvent have been obtained with the AM1 method.

Due to the rigidity of this system, the solvent effects on the geometry are small; in fact we also performed geometry optimizations with HF and B3LYP (both with the 6-311G(d) basis set), in vacuo and in water, and the values of absorption energies obtained at these geometries are very similar to that reported in the diagram of Figure 6. In contrast, the solvent effects are important to the absorption energies, as can be seen from data reported in Figure 6.

For all the methods, the calculations in vacuo provide values of transition energies larger than those obtained considering the solvent effect. Although the PCM improves the results, TD−HF and TD−DFT methods still overestimate the correct value of the transition energy. Also in this case, ZINDO performance is better than the ab initio results. In particular, the use of ZINDO with PCM allows us to obtain a value of the absorption energy very close to the experimental value.

This last example shows once more the effective potential of ZINDO/PCM to estimate the experimental data, providing results comparable and sometimes better than the ab initio methods and computationally less expensive.

## Summary

The IEF−PCM solvation model has been applied to the ZINDO semiempirical method. The latter is one of the most used methods to perform molecular calculations of absorption energies. In fact, despite its approximation, it was calibrated to give results quite close to the experimental data for a large series of organic molecules. When one is interested in transition energies for systems in solution, a good representation of the interaction between the solute and its surrounding is necessary. In the past years the IEF−PCM has been proven to be a very powerful model to represent the solvent response to the solute electronic excitation when coupled to ab initio methods. Here we have shown that the same good results can be obtained by coupling the IEF−PCM with ZINDO; this is an interesting result as ZINDO/PCM can become an important tool to describe the experimental trends of the spectra for many families of compounds, especially when the dimensions of the systems prevent from accurate ab initio approaches.

For the representation of the solute−solvent interaction, three different formulas of the electrostatic potential (and of the relative integrals) have been introduced in the INDO framework. In these formulas the potentials have been calculated (i) using a multipolar expansion (option *Multip*), (ii) using the ab initio expression of the integrals but neglecting those integrals that must be zero in the ZDO approximation (option *Integr*), (iii) using a point representation of the solute electronic charge (option *Chg*). The three formulas have been applied to the calculation of the PCM operators, introduced both in the SCF scheme and in the TDA approach developed to evaluate transition energies.

Three different classes of molecules have been selected to test the ZINDO/PCM model: three 7-aminocoumarin dyes, a pyridiniophenoxide betaine molecule, and the methylene blue dye. All the tests seem to confirm the validity of the model and of its approximations. Indeed, the results are in good agreement with the experimental data. For all the systems examined, the differences between the calculated and measured energies are lower than 0.1 eV in the polar solvents (for which the electrostatic term of the solute−solvent interaction is the most important one).

Comparing the three options for the calculation of the electrostatic potential, one can see that the values obtained for the excitation energies are close to each other, with differences less than 0.08 eV. This fact testifies that all three formulas, despite the different formulation, provide a quite good description of the potential.

Considering the timing, we have found that, despite the increase due to the PCM being more sensitive in semiempirical methods than in ab initio methods, the calculations remain much faster than the corresponding ab initio ones. In addition, we recall that for very large molecules a fast and efficient algorithm

has been developed for calculating the PCM terms,[40] which linearly scales with the number of the tesserae. This algorithm, even if it has not been used in this work, can be straightforwardly extended to the ZINDO/PCM model and it surely represents a further reason for making this model a valid computational tool.

Among the three formulas presented, we suggest as preferential choice the option *Multip*: its results are in fact the closer to the experimental data with respect to the other two options and its computational cost is the lowest.

The comparison with TD−HF and TD−DFT methods has also shown that for these molecular systems the semiempirical formulation of the PCM provides results more close to the experiments, despite its simplified form. In fact, for the betaine molecule the absorption energies obtained in acetone and acetonitrile with the TD−DFT/PCM method are 0.3−0.4 eV lower than the experimental energies, instead of the 0.02−0.05 eV obtained with ZINDO/PCM. Also for the methylene blue, the calculations in water with the TD−HF and TD−DFT methods are shown to be worse than that performed with ZINDO, the differences being with respect to the experimental value of the order of 0.9, 0.4, and 0.01 eV, respectively.

In conclusion, the examples reported in this paper show that the ZINDO/PCM method can accurately describe the phenomenon of the electronic absorption in solution and thus it can be seen as a promising method to study the absorption transitions of large systems in solution.

**Acknowledgment.** Francesca Ingrosso is acknowledged for providing the DFT calculations of the coumarin 3 and Paula Homem de Mello for performing the calculations of the methylene blue dye.

## References and Notes

(1) Miertus, S.; Scrocco, E.; Tomasi, J. *J. Chem. Phys.* **1981**, *55*, 117.
(2) Tomasi, J.; Persico, M. *Chem. Rev.* **1994**, *94*, 2027.
(3) Bacon, A. D.; Zerner, M. C. *Theo. Chim. Acta* **1979**, *53*, 21.
(4) Correa de Mello, P.; Hehenberger, M.; Zerner, M. C. *Int. J. Quantum Chem.* **1982**, *21*, 251.
(5) Zerner, M. C. *J. Chem. Phys.* **1975**, *62*, 7, 2788.
(6) Zerner, M. C. *Reviews in Computational Chemistry*, Lipkowitz, K. B., Boyd, D. B.; VCH Publishing: New York, 1991; Vol.2, pp 313−366.
(7) Tomasi, J.; Cammi, R.; Mennucci, B.; Cappelli, C.; Corni, S. *Phys. Chem. Chem. Phys.* **2002**, *4*, 5697.
(8) Cancès, E.; Mennucci, B. *J. Mater. Chem.* **1998**, *23*, 309.
(9) Cancès, E.; Mennucci, B.; Tomasi, J. *J. Chem. Phys.* **1997**, *107*, 3031.
(10) Mennucci, B.; Cancès, E.; Tomasi, J. *J. Phys. Chem. B* **1997**, *101*, 10506.
(11) Onsager, L. *J. Am. Chem. Soc.* **1936**, *58*, 1486.
(12) Karelson, M. M.; Zerner, M. C. *J. Phys. Chem.* **1992**, *96*, 6949.
(13) Albert, I. D. L.; Marks, T. J.; Ratner, M. A. *J. Phys. Chem.* **1996**, *100*, 9714.
(14) Yu, J.; Zerner, M. C. *J. Chem. Phys.* **1994**, *100*, 10, 7487.
(15) Kölle, C.; Jug, K. *J. Comput. Chem.* **1997**, *18*, 1, 1.
(16) Baraldi, I.; Momicchioli, F.; Ponterini, G.; Vanossi, D. *Chem. Phys.* **1998**, *238*, 353.
(17) Manas, E. S.; Wright, W. W.; Sharp, K. A.; Friedrich, J.; Vanderkooi, J. M. *J. Phys. Chem. B* **2000**, *104*, 6932.
(18) Vivian, T. J.; Callis, P. R. *Biophys. J.* **2001**, *80*, 2093.
(19) Fox, T.; Rösch, N.; Zauhar, R. J. *J. Comput. Chem.* **1993**, *14*, 3, 253.
(20) Broo, A.; Pearl, G.; Zerner, M. C. *J. Phys. Chem. A* **1997**, *101*, 2478.
(21) Tomasi, J.; Bonaccorsi, R.; Cammi, R. *Theoretical models of Chemical Bonding*, Maksić, Z. B., Ed.; Springer-Verlag, Berlin, Heidelberg, 1991, 229−268.
(22) Margenau, H.; Kestner, N. R. *Theory of intermolecular forces*, Wiley: New York, 1969.
(23) Böttcher, C. F. J.; Bordewijk, P. *Theory of electric polarization*, Elsevier: Amsterdam, 1978.
(24) Williams, D. E.; Yan, J. M. *Adv. At. Mol. Phys.* **1988**, *23*, 87.
(25) Frisch, M. J.; Trucks, G. W.; Schlegel, H. B.; Scuseria, G. E.; Robb, M. A.; Cheeseman, J. R.; Montgomery, J. A. Jr.; Vreven, T.; Kudin, K. N.; Burant, J. C.; Millam, J. M.; Iyengar, S. S.; Tomasi, J.; Barone, V.; Mennucci, B.; Cossi, M.; Scalmani, G.; Rega, N.; Petersson, G. A.; Nakatsuji, H.; Hada, M.; Ehara, M.; Toyota, K.; Fukuda, R.; Hasegawa, J.; Ishida, M.; Nakajima, T.; Honda, Y.; Kitao, O.; Nakai, H.; Klene, M.; Li, X.; Knox, J. E.; Hratchian, H. P.; Cross, J. B.; Adamo, C.; Jaramillo, J.; Gomperts, R.; Stratmann, R. E.; Yazyev, O.; Austin, A. J.; Cammi, R.; Pomelli, C.; Ochterski, J. W.; Ayala, P. Y.; Morokuma, K.; Voth, G. A.; Salvador, P.; Dannenberg, J. J.; Zakrzewski, V. G.; Dapprich, S.; Daniels, A. D.; Strain, M. C.; Farkas, O.; Malick, D. K.; Rabuck, A. D.; Raghavachari, K.; Foresman, J. B.; Ortiz, J. V.; Cui, Q.; Baboul, A. G.; Clifford, S.; Cioslowski, J.; Stefanov, B. B.; Liu, G.; Liashenko, A.; Piskorz, P.; Komaromi, I.; Martin, R. L.; Fox, D. J.; Keith, T.; Al-Laham, M. A.; Peng, C. Y.; Nanayakkara, A.; Challacombe, M.; Gill, P. M. W.; Johnson, B.; Chen, W.; Wong, M. W.; Gonzalez, C.; Pople, J. A. *Gaussian 03*, Revision B.01; Gaussian, Inc.: Pittsburgh, PA, 2003.
(26) Pople, J. A.; Santry, D. P.; Segal, G. A. *J. Chem. Phys.* **1965**, *43*, 8129.
(27) Dewar, M. J. S.; Thiel, W. *Theor. Chim. Acta* **1977**, *46*, 89.
(28) Rauhut, G.; Clark, T.; Steinke, T. *J. Am. Chem. Soc.* **1993**, *115*, 9174.
(29) Dewar, M. J. S.; Thiel, W. *J. Am. Chem. Soc.* **1977**, *99*, 4899.
(30) Dewar, M. J. S.; Zoebisch, E. G.; Healy, E. F.; Stewart, J. J. P. *J. Am. Chem. Soc.* **1985**, *107*, 3902.
(31) Stewart, J. J. P. *J. Comput. Chem.* **1989**, *10*, 209, 221.
(32) McWeeny, R. *Methods of Molecular Quantum Mechanics*, 2nd ed.; Academic: London, 1992.
(33) Foresman, J. B.; Head-Gordon, M.; Pople, J. A.; Frisch, M. J. *J. Phys. Chem.* **1992**, *96*, 135.
(34) Parkinson, W. A.; Zerner, M. C. *J. Chem. Phys.* **1989**, *90*, 10, 5606.
(35) Cramer, C. J.; Truhlar, D. G. *Chem. Rev.* **1999**, *99*, 2161.
(36) Mennucci, B.; Cammi, R.; Tomasi, J. *J. Chem. Phys.* **1998**, *109*, 2978.
(37) Cammi, R.; Mennucci, B. *J. Chem. Phys.* **1999**, *110*, 20, 9877.
(38) Cammi, R.; Mennucci, B.; Tomasi, J. *J. Phys. Chem. A* **2000**, *104*, 5631.
(39) Ridley, J. E.; Zerner, M. C. *Theor. Chim. Acta*, **1973**, *32*, 111.
(40) Scalmani, G.; Barone, V.; Kudin, K. N.; Pomelli, C. S.; Scuseria, G. E.; Frisch, M. J. *Theor. Chem. Acc.* **2004**, *111*, 90.
(41) Jones, G., II; Griffin, S. F.; Choi, C.; Bergmark, W. R. *J. Org. Chem.* **1984**, *49*, 2705.
(42) Jones, G., II; Jackson, W. R.; Choi, C.; Bergmark, W. R. *J. Phys. Chem.* **1985**, *89*, 294.
(43) Cave, R. J.; Burke, K.; Castner, E. W., Jr. *J. Phys. Chem. A* **2002**, *106*, 9294.
(44) Cave, R. J.; Castner, E. W., Jr. *J. Phys. Chem. A* **2002**, *106*, 12117.
(45) Reichardt, C. *Chem. Rev.* **1994**, *94*, 2319.
(46) Bartkowiak, W.; Lipiński, J. *J. Phys. Chem. A* **1998**, *102*, 5236.
(47) Gonzalez, D.; Neiland, O.; Rezende, M. C. *J. Chem. Soc., Perkin Trans. 2*, **1999**, *713*.
(48) Lobaugh, J.; Rossky, P. J. *J. Chem. Phys. A* **2000**, *104*, 899.
(49) Ishida, T.; Rossky, P. J. *J. Phys. Chem. A* **2001**, *105*, 9379.
(50) Reichardt, C. *Solvents and Solvent Effects in Organic Chemistry*, 3rd ed.; VCH: Weinheim, 2003.
(51) http://ntp-server.niehs.nih.gov/htdocs/Chem_Background/ExecSumm/MethyleneBlue.html
(52) Gessner, F.; Schmitt, C. C.; Neumann, M. G. *Langmuir* **1994**, *10*, 3749.
(53) Bujdák, J.; Komadel, P. *J. Phys. Chem. B* **1997**, *101*, 9065.
(54) Neumann, M. G.; Gessner, F.; Schmitt, C. C.; Sartori, R. *J. Colloid Interface Sci.* **2002**, *255*, 254.
(55) Neumann, M. G.; Gessner, F.; Cione, A. P. P.; Sartori, R.; Schmitt Cavalheiro, C. C. *Quimica Nova* **2000**, *23*, 818.